Disruption of Growth Factor Receptor–Binding Protein 10 in the Pancreas Enhances β-Cell Proliferation and Protects Mice From Streptozotocin-Induced β-Cell Apoptosis

Jingjing Zhang,[1,2] Ning Zhang,[3] Meilian Liu,[2] Xiuling Li,[4] Lijun Zhou,[2] Wei Huang,[1] Zhipeng Xu,[1] Jing Liu,[2] Nicolas Musi,[3] Ralph A. DeFronzo,[3] John M. Cunningham,[4] Zhiguang Zhou,[1,5] Xin-Yun Lu,[2] and Feng Liu[1,2]

Defects in insulin secretion and reduction in β-cell mass are associated with type 2 diabetes in humans, and understanding the basis for these dysfunctions may reveal strategies for diabetes therapy. In this study, we show that pancreas-specific knockout of growth factor receptor–binding protein 10 (Grb10), which is highly expressed in pancreas and islets, leads to elevated insulin/IGF-1 signaling in islets, enhanced β-cell mass and insulin content, and increased insulin secretion in mice. Pancreas-specific disruption of Grb10 expression also improved glucose tolerance in mice fed with a high-fat diet and protected mice from streptozotocin-induced β-cell apoptosis and body weight loss. Our study has identified Grb10 as an important regulator of β-cell proliferation and demonstrated that reducing the expression level of Grb10 could provide a novel means to increase β-cell mass and reduce β-cell apoptosis. This is critical for effective therapeutic treatment of both type 1 and 2 diabetes. ***Diabetes*** **61:3189–3198, 2012**

To maintain glucose homeostasis, pancreatic β-cells are able to adapt their insulin- secretory capacity in response to altered physiological and pathological demands. A key mechanism contributing to this adaptability is enhanced insulin secretion from existing β-cells and increased β-cell mass (1,2). β-Cell mass is the sum of β-cell size, the rate of cell proliferation/differentiation, and the difference between β-cell neogenesis and apoptosis (3). Reduction in β-cell mass is associated with type 2 diabetes in humans (4). Therefore, expansion of the β-cell mass from endogenous sources, either in vivo or in vitro, represents a highly significant research area for developing specific treatment of human diabetes.

From the [1]Metabolic Syndrome Research Center, Diabetes Center, Institute of Metabolism and Endocrinology, the Second Xiangya Hospital, Central South University, Changsha, Hunan, China; the [2]Department of Pharmacology, University of Texas Health Science Center at San Antonio, San Antonio, Texas; the [3]Department of Medicine, University of Texas Health Science Center at San Antonio, San Antonio, Texas; the [4]Department of Hematology/Oncology, St. Jude Children's Research Hospital, Memphis, Tennessee; and the [5]Key Laboratory of Diabetes Immunology, Ministry of Education, Diabetes Center, Institute of Metabolism and Endocrinology, the Second Xiangya Hospital, Central South University, Changsha, Hunan, China.
Corresponding author: Feng Liu, liuf@uthscsa.edu.
Received 27 February 2012 and accepted 26 June 2012.
DOI: 10.2337/db12-0249
This article contains Supplementary Data online at http://diabetes.diabetesjournals.org/lookup/suppl/doi:10.2337/db12-0249/-/DC1.

See accompanying commentary, p. 3066.

Growth factor receptor–binding protein 10 (Grb10) is a pleckstrin homology and Src homology 2 (SH2) domain-containing protein that interacts with several receptor tyrosine kinases, including the insulin receptor (IR) and the IGF-1 receptor (IGF1R) (5,6). The interaction between Grb10 and these receptors negatively regulates insulin and IGF-1 signaling in cultured cells (7–9) and in vivo (10,11). Grb10 negatively regulates insulin or IGF-1 signaling by binding to the kinase domain of the tyrosine-phosphorylated IR or IGF1R, mainly via its SH2 domain and partly a region between the pleckstrin homology domain and the SH2 domain (BPS) (9,12–14). Grb10 is expressed in insulin target tissues such as fat and muscle, but the highest expression of this protein is in pancreas of adult mice (11). Although disruption of the Grb10 gene in all tissues (except the brain) significantly increases the size of pancreas in mice (11,15), the underlying mechanisms are unknown. It is also unclear whether Grb10 has an autonomous role in regulating pancreatic cell mass and β-cell function. In this study, we report the establishment and characterization of the first tissue-specific Grb10 knockout mice. In addition, we demonstrate that pancreas-specific deletion of the Grb10 gene enhanced β-cell proliferation and improved glucose tolerance under high-fat diet (HFD) feeding condition. Knockout of Grb10 in the pancreas protects mice from streptozotocin (STZ)-induced apoptosis, suggesting that suppressing the expression levels of Grb10 in the pancreas could be a promising approach for increasing β-cell mass and improving β-cell function.

RESEARCH DESIGN AND METHODS

Generation of Grb10 conditional knockout mice in the pancreas. A 100-kb region of the Grb10 gene was isolated from a mouse bacterial artificial chromosome library (Invitrogen/Life Technologies, Grand Island, NY) and the targeting vector, in which exon 3 of the Grb10 gene is flanked by *loxP* sites (Grb10*loxP*), was constructed by using standard molecular biology techniques. The targeting vector was linearized with Kpn1 and electroporated into the 129/SVEV embryonic stem cell line. Positive clones were selected by G418 (300 μg/mL) and ganciclovir (2 μmol/L) double resistance and verified by Southern blot. Clones of Grb10$^{loxP/+}$ embryonic stem cells that undergo homologous recombination and possessed a single integration event were used to microinject C57BL/6 blastocysts. Chimeric mice were mated with C57BL/6 mice, and germline transmission of the floxed Grb10 allele was confirmed by Southern blot and PCR genotyping. The Neo cassette was removed by crossing the floxed mice carrying the targeting vector with FLP mice (The Jackson Laboratory) expressing FRT in their germline. Grb10 is an imprinted gene and is paternally expressed in the brain and maternally expressed in all other tissues (16). Thus, female homozygous Grb10 floxed mice were used to breed with male heterozygous PDX-Cre mice, which led to the generation of pancreas-specific Grb10 knockout mice, hereafter referred to as pGrb10KO mice, and the Grb10 flox$^{+/-}$ wild-type (WT) littermates. Because Grb10

expression in the brain is paternally imprinted, our breeding strategy does not affect Grb10 expression in the brain. All animals were housed in specific pathogen-free facilities, maintained on a 12-h light/dark cycle, and fed standard rodent chow at the Department of Laboratory Animal Resources in the University of Texas Health Science Center at San Antonio and the Animal Care Center in the Second Xiangya Hospital of Central South University. All protocols for animal use were approved by the University of Texas Health Science Center at San Antonio Animal Care and Use Committee and the Second Xiangya Hospital Animal Care and Use Committee of Central South University.

Body weight, food intake, body composition, glucose, and insulin tolerance tests. Mice were fed a normal diet (19% protein; 5% fat; 5% fiber; 7912-012809M; Irradiated, Madison, WI) or an HFD (60% fat, 20% carbohydrate, 20% protein; D12492; Research Diets, New Brunswick, NJ) for 16 weeks. Mouse body weight and food intake were monitored at the same time on a weekly basis from 4 weeks onward. To check body composition, mice were i.p. injected with Avertin (250 mg/kg animal body weight). Fat and lean tissue masses and bone mineral content were determined using dual-energy X-ray absorptiometry (Lunar PIXImus 2; GE Medical Systems, Madison, WI). Glucose tolerance tests (GTT) were performed by injection of glucose (2 g/kg body weight i.p.) into overnight fasted mice. Blood was withdrawn from the tail vein at 0, 15, 30, 60, and 120 min after glucose administration. Insulin tolerance tests were performed by injection of insulin (0.75 g/kg body weight i.p.) into nonfasted mice. Blood was withdrawn from the tail vein at 0, 15, 30, and 60 min after insulin administration. Serum glucose levels were determined using a glucometer (One Touch; Bionime Corp.). Serum insulin levels were determined by insulin ultrasensitive enzyme immunoassay (Alpco Diagnostics, Slemm, NH).

Hyperglycemic clamp. Hyperglycemic clamps were performed in conscious male pGrb10KO mice and control WT littermates at 3 months of age (n = 4 to 5/group). In brief, mice were fasted overnight and anesthetized by an intraperitoneal injection of ketamine (100 mg/kg body weight) and xylazine (10 mg/kg body weight). An indwelling catheter was inserted in the right internal jugular vein 4 to 5 days before clamp experiments. Mice were housed in individual cages and monitored for postoperative recovery and weight gain. Following overnight fast, a 2-h hyperglycemic clamp was conducted in conscious mice with a variable infusion of 20% glucose to raise and maintain plasma glucose concentration at ~300 mg/dL. Blood samples (40 μL) were collected at 5–10-min intervals for the measurement of plasma glucose and insulin levels.

Islet isolation, Western blot analysis, and insulin granule counting. Mouse islets were isolated by collagenase digestion of the pancreas according to the procedures described (17–19). In brief, overnight-fasted male pGrb10KO mice and WT littermates (2–6 months old) were anesthetized by intraperitoneal injection of avertin (1 mL/40 g body weight). Mouse pancreas was inflated by injection of 3 mL of a collagenase P solution (Sigma Chemical, St. Louis, MO; 1 mg/mL in Hank's buffered salt solution). Pancreases were removed and incubated at 37°C for about 12 min to allow complete digestion. Digestion was stopped by the addition of 30 mL of Hank's buffered salt solution, followed by washing the pancreases with 20 mL RPMI-1640 medium three times. Isolated islets were selected with the aid of a pipette under a stereoscopic microscope from the medium and maintained in RPMI-1640 with or without 10% FBS or HEPES-balanced Krebs-Ringer bicarbonate buffer (119 mmol/L NaCl, 4.74 mmol/L KCl, 2.54 mmol/L $CaCl_2$, 1.19 mmol/L $MgCl_2$, 1.19 mmol/L KHPO, 25 mmol/L $NaHCO_3$, and 10 mmol/L HEPES [pH 7.4]) containing 0.5% BSA at 37°C.

For insulin and IGF-1 signaling studies, the freshly isolated islets (30 islets/experiments) were serum-starved for 2 h and then treated with or without 100 nmol/L insulin for 30 min or 100 nmol/L IGF-1 for 30 min. For mammalian target of rapamycin (mTOR) signaling studies, freshly isolated islets (50 islets/experiment) were serum-starved for 2 h and then treated with 100 nmol/L insulin with or without 100 nmol/L wortmannin for 30 min. Islets were lysed, and insulin-stimulated phosphorylation of Akt at Thr^{308} and Ser^{473}, extracellular signal–regulated, mitogen-activated protein kinase 1 and 2 (ERK1/2) at Thr^{202}/Tyr^{204}, p70S6K at Thr^{389}, and 4E-BP1 at $Thr^{37/46}$, as well as the protein levels of these insulin/IGF-1 or mTOR signaling molecules, were determined by Western blot using specific antibodies. Antibodies and phosphoantibodies to Akt, ERK1/2, S6K, and 4E-BP1 were purchased from Cell Signaling Technology or Millipore (for ERK1/2). The antibody to Grb10 was described previously (8). Wortmannin was purchased from Sigma Chemical.

For insulin granule counting, islets were isolated, fixed with 1% glutaraldehyde, and then embedded in epon. Blocks of tissue (0.1–1.5 mm^3) were osmicated in 0.1 mol/L sodium cacodylate buffer (pH 7.4) containing 1% OsO_4 for 1 h at room temperature, rinsed in cacodylate buffer, and then rinsed in distilled water before they were stained in 2% uranyl acetate double-distilled water for 1 h. Sections were dehydrated in graded alcohol and placed in 100% propylene oxide. The blocks were incubated in epon–propylene-oxide (1:1) overnight at room temperature and then changed to 100% epon and polymerized overnight. Sections (90 nm) were cut on a Reichert-Jung Ultracut E microtome, collected on slot grids, and stained with 2% uranyl acetate and lead citrate. The pictures were captured by Jeol1230 Transmitted Electronic Microscope (JEOL, Peabody, MA).

Islet proliferation assays. Male mice (2 months old; n = 3 to 4/genotype) were injected intraperitoneally with 100 mg/kg of 5-bromo-2′ deoxyuridine (BrdU; Roche Molecular Biochemicals, Indianapolis, IN) and killed 16 h after injection. Pancreases were isolated, fixed, and sectioned. Pancreas slices were analyzed by double staining with anti-BrdU (Millipore) and anti-insulin (Santa Cruz Biotechnology) antibodies. Insulin-positive β-cells (>2,500 β-cells/pancreas) were counted, and the percentage of BrdU- and insulin-double positive nuclei to total insulin-positive nuclei was determined for both pGrb10KO mice and their WT control mice. Quantification of total BrdU-positive cell numbers was done by using an unbiased stereological method to ensure that the same BrdU-labeled cell is not counted twice on adjacent sections and that the area of the pancreatic sections counted for each animal are consistent.

Immunohistochemistry of pancreas. The immunohistochemistry experiments were carried out as previously described (20), with some modifications. In brief, pancreases obtained from 16-week-old male pGrb10 KO mice and their Grb10 WT littermates, cleared of fat and spleen, weighted, and fixed in ice-cold 4% paraformaldehyde (Electron Microscopy Sciences, Fort Washington, PA). The fixed tissues were embedded in Optimal Cutting Temperature Compound (Ted Pella, Inc.) and cut into 10-μm sections using a cryostat or a microtome. The slices were rehydrated, permeabilized, and stained with specific antibodies (Grb10 [homemade], 1:400; Insulin [Santa Cruz Biotechnology], 1:100; or E-cadherin [BD Biosciences], 1:50). The cell nuclei were determined by 4′,6-diamidino-2-phenylindole staining.

The analysis of islet mass and β-cell size. Male mouse pancreases were cut into 10-μm sections systematically through pancreatic head-to-tail axis, and sections were selected between every 200 μm. Eight sections per mouse were picked. Mouse pancreatic slices were stained with an anti-insulin antibody. Images of pancreas slices were viewed by an Olympus inverted microscope (IX7) and captured with a Sport II digital camera (Olympus, Japan). All insulin-positive β-cell clusters (islets) were loosely traced, and the insulin-immunoreactive areas were determined by use of the threshold option (21). Total tissue areas were quantified with the threshold option to select the stained areas but not unstained areas (white space). The islet area (in square micrometers) and the area of each section were determined with Image J software (National Institutes of Health). Four to eight sections of each pancreas were covered by accumulating images from eight nonoverlapping fields of 1.5×10^6 μm^2. Analyses of β-cell area and size were performed using Image J software (National Institutes of Health) or the Image-Pro Plus software (Version 5.0; Media Cybernetics, Inc). β-Cell mass was calculated by insulin-positive area/total pancreas area times pancreas weight (17,22,23).

STZ-induced β-cell apoptosis and transferase-mediated dUTP nick-end labeling assays. Male WT and pGrb10KO mice (2 months old) were injected once per day with freshly prepared STZ solution (0.8% in 0.1 mol/L sodium citrate [pH 4.5]) for 5 days (75 mg/kg i.p.). Blood glucose levels and body weight were examined every 3 days at the same time (12 P.M. every day). Twenty-two days later, mice were killed, and serum insulin levels, islet mass, and pancreas weight of the mice were determined. For acute STZ treatment experiments, male mice were injected with STZ twice daily (at 0 and 24 h) and killed 16 h later. Dewaxed paraffin sections of the pancreas were labeled with an in situ cell death detection kit (Roche) and insulin antibody, and STZ-induced apoptosis was determined by immunofluorescence using a Nikon TE2000 microscope (Nikon). Four mice per group were used for transferase-mediated dUTP nick-end labeling (TUNEL) assays, and at least five islets (500–1,000 β-cells) were counted for each mouse.

Statistics. Quantification of the relative increase in insulin-stimulated protein phosphorylation was performed by analyzing Western blots using Scion Image software and was normalized with the amount of protein expression in each experiment. Statistical analysis of the data was performed by using unpaired Student t test or ANOVA (one-way repeated-measure ANOVA or two-way ANOVA with post hoc Bonferroni test). Statistical significance was set at P values of <0.05, <0.01, and <0.001.

RESULTS

Generation and characterization of pGrb10KO mice. Grb10 floxed construct was generated by insertion of loxP sites at both ends of exon 3 of the Grb10 gene (Fig. 1*A*). Exon/intron boundary analysis revealed that deletion of this exon causes a frame shift and thus a null mutant of Grb10. The floxed Grb10 allele was confirmed by Southern blot (Fig. 1*B*) and PCR genotyping (data not shown). The Neo cassette was removed by crossing the floxed mice with the FLP mice expressing FRT in their germline (The

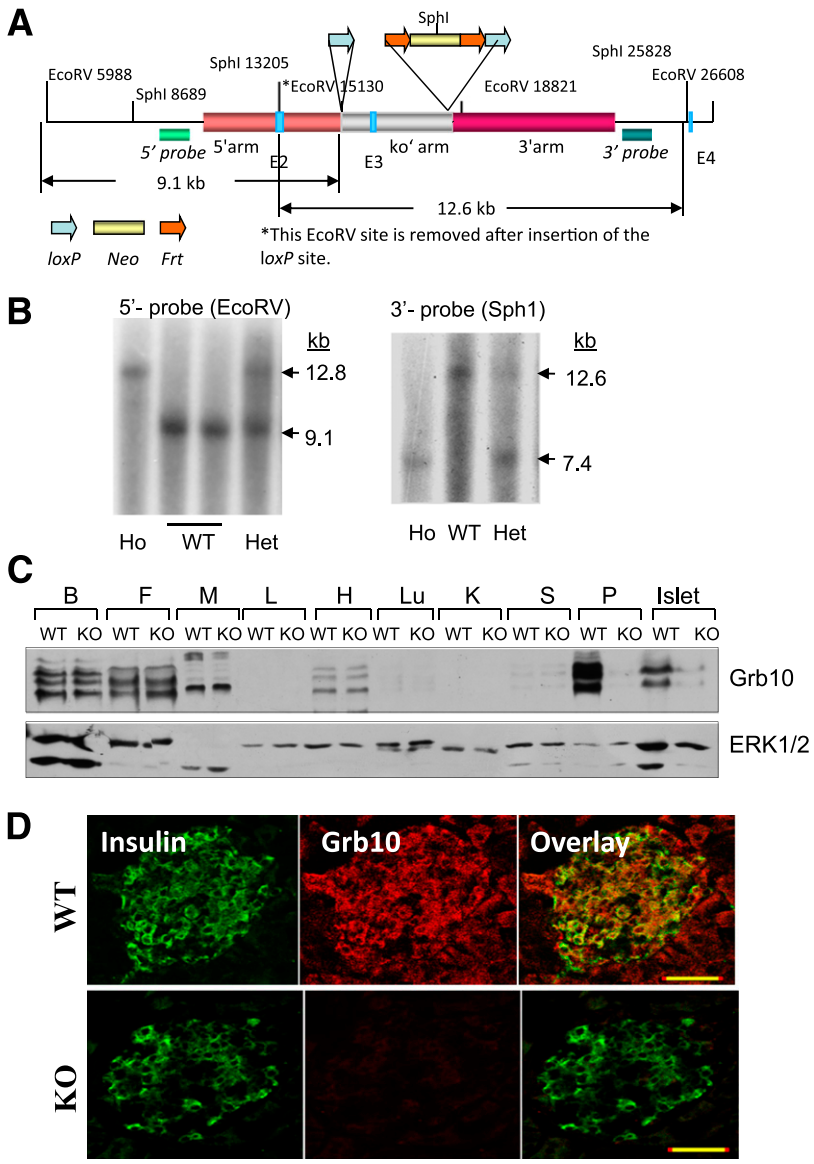

FIG. 1. Generation of pGrb10KO mice. *A*: Schematic diagram of the strategy used to target the mouse *Grb10* locus. The targeting vector is shown. *B*: Southern blot analysis of WT, homozygous (Ho), and heterozygous (Het) Grb10 floxed mice. Genomic DNA extracted from the mice was digested with *Eco*RV and gel-fractionated. The blot was hybridized with 5′- or 3′-probe as indicated. *C*: Western blot analysis of tissues from pGrb10KO and control mice to confirm the successful knockout of Grb10 in the pancreas. ERK1/2 is shown as a loading control. *D*: The pancreases of pGrb10KO (KO) and WT littermates were sectioned at 10 μm by using a cryostat. Protein expression in pancreas sections was determined using goat anti-insulin (C-12) antibody (Santa Cruz Biotechnology) and a homemade, affinity-purified rabbit polyclonal antibody to Grb10 (8). The slide images were obtained using a laser confocal fluorescence microscope. Scale bars, 40 μm. B, brain; F, fat; H, heart; K, kidney; L, liver; Lu, lung; M, muscle; P, pancreas; S, spleen. (A high-quality digital representation of this figure is available in the online issue.)

Jackson Laboratory). Grb10 is an imprinted gene and is maternally expressed in peripheral tissues (6). Thus, we bred female homozygous Grb10 floxed mice with male heterozygous PDX-Cre$^{+/-}$ mice, which led to Cre-mediated deletion of the Grb10 gene specifically in the pancreas but not other tissues including the brain (pGrb10KO; Fig. 1*C* and Supplementary Fig. 1*B* and *C*). Western blot analysis also revealed that Grb10 is highly expressed in mouse pancreas and islets (Fig. 1*C* and Supplementary Fig. 1*A*). By immunohistochemistry studies, we found that Grb10 protein is expressed in islets and neighboring cells in the pancreas, and its signal is highly colocalized with insulin-staining cells (Fig. 1*D*, *top panel*). This further confirms that Grb10 is expressed in pancreatic β-cells. No Grb10 signal was detected in the pancreatic section of the pGrb10KO mice (Fig. 1*D*, *bottom panel*), demonstrating the successful deletion of the Grb10 gene in the pancreas of the knockout mice. Consistent with the finding of Smith et al. (10), our breeding strategy had no effect on Grb10 expression in the hypothalamus (Supplementary Fig. 1*B* and *C*).

Pancreas-specific knockout of Grb10 had little effect on mouse body composition, food intake, and body weight compared with WT littermates (Supplementary Figs. 2 and 3), but significantly increased pancreas tissue weight (Fig. 2*A*). Whereas the β-cell size did not differ between these two strains fed with normal chow diet, the male pGrb10KO mice displayed more β-cell mass than WT mice (Fig. 2*B* and *C*). By 4′,6-diamidino-2-phenylindole/insulin/BrdU triple staining of pancreatic sections, we found that the rate of BrdU incorporation into β-cell cells was quite slow in WT

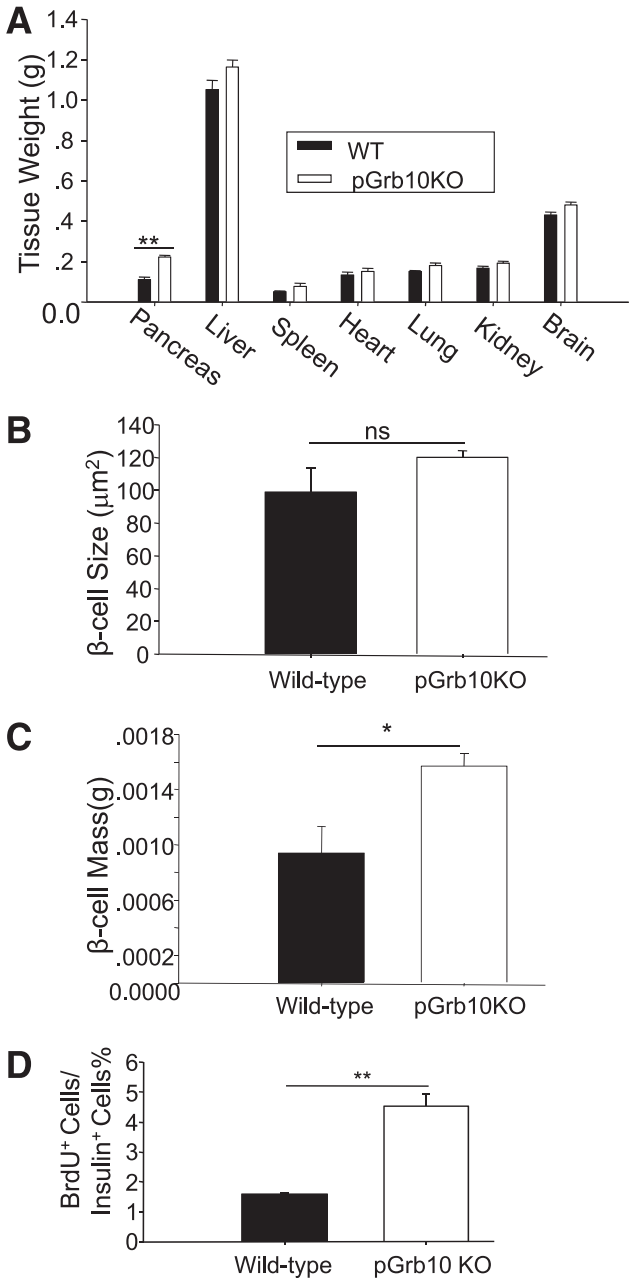

FIG. 2. Pancreatic knockout of Grb10 increases pancreas weight, β-cell mass, and BrdU incorporation rate in β-cells. *A*: Mouse tissues were isolated from 5-month-old male WT (n = 6) and pGrb10KO mice (n = 5) fed with normal diet and weighed by electronic balance. *B*: β-Cell size between male pGrb10KO mice and WT littermates (n = 4/group; >500 cells were counted per slide) was measured using Image-Pro Plus software (Version 5.0; Media Cybernetics, Inc). *C*: Average β-cell mass between 5-month-old male pGrb10KO mice and WT littermates fed with normal diet (WT: n = 7; pGrb10 KO: n = 4). *D*: Knockout of Grb10 increased β-cell proliferation as determined by BrdU cell proliferation assay. BrdU was injected into 2-month-old male mice (100 mg/kg), and mice were killed 16 h after injection. More than 2,500 insulin-positive cell nuclei were counted per mouse under a Nikon TE2000 microscope (Nikon; WT: n = 3; pGrb10KO: n = 4). Black bars, Grb10 flox$^{+/-}$; white bars, pGrb10 KO. All data represent mean ± SEM. *P < 0.05; **P < 0.01 (t test).

control mice, ~2,500 insulin-positive cells per individual animal (Fig. 2*D*). BrdU-positive cells were significantly increased in the pancreatic sections of the pGrb10KO mice (Fig. 2*D*). Taken together, these results suggest that endogenous Grb10 negatively regulates β-cell proliferation.

Pancreas-specific disruption of the Grb10 gene improves glucose tolerance and insulin secretion. Under normal chow-feeding conditions, the pGrb10KO mice showed a slightly lower fasting blood glucose levels and displayed better glucose tolerance compared with the WT littermates (Fig. 3*A*). However, there was no overall significant difference in insulin tolerance between pGrb10KO and WT littermates. On an HFD, the pGrb10 KO mice and their WT littermates showed similar body weight, food intake, and body composition (Supplementary Fig. 3). Although insulin tolerance tests showed similar insulin tolerance between the two strains (data not shown), the pGrb10KO mice displayed significantly better glucose tolerance compared with WT littermates (Fig. 3*B*), suggesting improved insulin secretion in the pGrb10KO mice. Under normal diet, both WT and pGrb10KO mice exhibited relatively normal glucose levels. Although pGrb10KO mice showed slightly lower glucose levels, they were not hypoglycemic (Fig. 3*A*). After challenged with 60% HFD for 16 weeks, WT mice showed high glucose levels, but pGrb10KO mice still maintain comparably lower serum glucose (Fig. 3*B*). Consistent with these findings, hyperglycemic clamp studies revealed that pGrb10KO mice exhibited higher glucose infusion rate (GIR) compared to wild-type littermates (Fig. 3*C*). The insulin secretion rate of the pGrb10KO mice was also higher than that of the wild-type control mice during the hyperglycemic clamp studies (Fig. 3*D*).

Targeted deletion of the Grb10 gene in pancreas enhances β-cell mass and insulin/IGF-1 and mTOR signaling in islets. To elucidate the mechanism by which disruption of Grb10 expression leads to increased insulin secretion in mice, we examined total β-cell mass and individual β-cell size. The male pGrb10KO mice displayed higher β-cell mass than that of the WT littermates (~0.003 vs. 0.001–0.0015 g/mouse) (Fig. 4*A*). Consistent with these results, transmission electron microscopy studies showed increased insulin granules in β-cells of the pGrb10KO mice compared with WT littermates (Fig. 4*B*; 12.47 ± 0.34/μm^2 vs. 9.25 ± 0.52/μm^2; P < 0.001). However, the sizes of individual β-cells are similar between these two strains (Fig. 4*C*), suggesting that the increased β-cell mass is mainly due to enhanced cell proliferation in the pGrb10KO mice. This finding is also consistent with the results from the BrdU staining experiments (Fig. 2*D*). By Western blot, we found that insulin and IGF-1 had a greater effect on the phosphorylation of Akt Thr^{308} and ERK1/2 Thr^{202}/Tyr^{204} in islets isolated from HFD-fed pGrb10KO mice compared with their WT littermates (Fig. 4*D*). Insulin-stimulated phosphorylation of Akt Thr^{308} and Ser^{473}, ERK1/2 Thr^{202}/Tyr^{204}, p70S6K Thr^{389}, and 4E-BP1 Thr$^{37/46}$ was enhanced in pGrb10KO mice compared with WT mice and could have been blocked by wortmannin (Fig. 4*E*). Similar results were also observed in mice fed with normal diet (data not shown).

Pancreas-specific knockout of Grb10 protects mice from STZ-induced diabetes. To determine whether pancreas-specific deletion of the Grb10 gene has a beneficial effect on diabetes, we investigated the effect of low-dose STZ treatment on β-cell damage in 2-month-old pGrb10 KO mice and WT littermates. STZ treatment greatly increased serum glucose levels in WT mice, and the STZ-induced hyperglycemic effect was significantly reduced in the pGrb10KO mice (Fig. 5*A*). Pancreas-specific knockout of Grb10 also significantly protected mice from STZ-induced body weight loss (Fig. 5*B*), which is a typical characteristic of diabetes. Furthermore, the male pGrb10KO mice showed

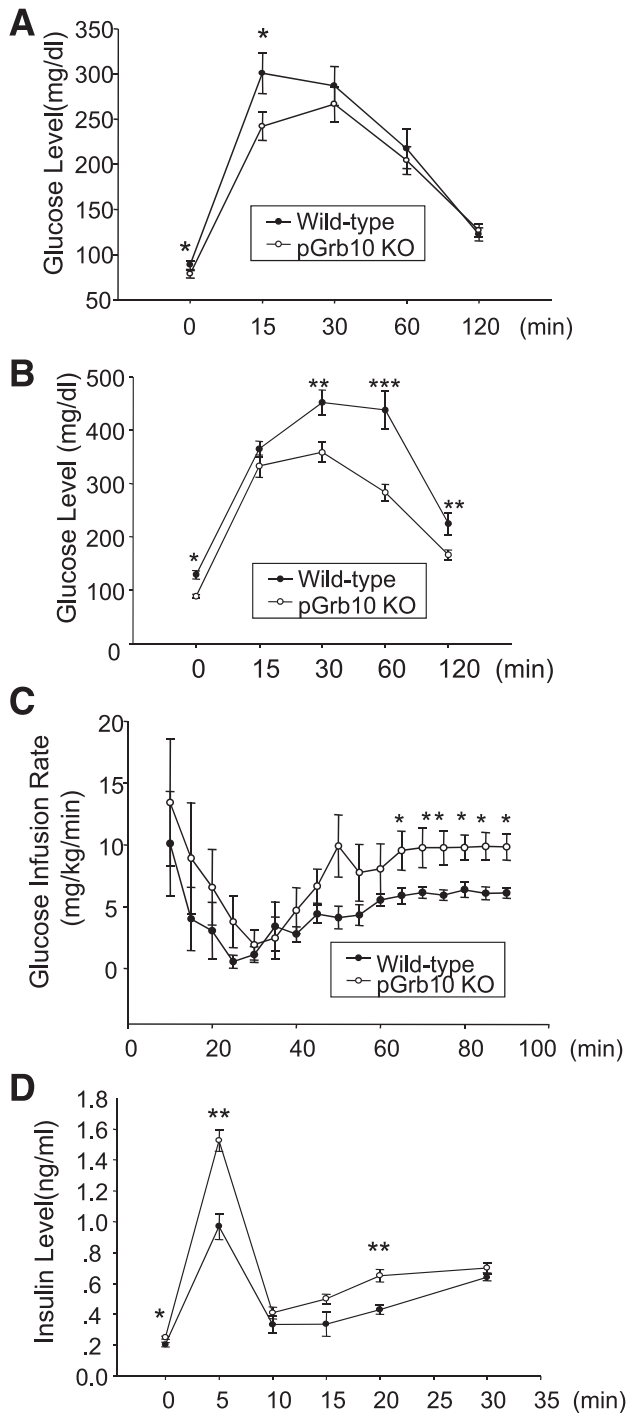

FIG. 3. Pancreatic knockout of Grb10 increases glucose tolerance and insulin secretion. *A*: GTT was performed in 5-month-old male pGrb10KO mice (n = 9) and age-matched WT littermates (n = 8) fed with normal diet. Blood glucose was withdrawn from the tail vein at 0, 15, 30, 60, and 120 min after intraperitoneal injection of glucose (2 g/kg body weight) and measured using a glucometer. *B*: GTT was performed on overnight-fasted male pGrb10KO mice and WT littermates (WT: n = 11; pGrb10KO: n = 9) fed with 60% HFD for 16 weeks. Blood glucose after intraperitoneal injection of glucose (2 g/kg body weight) was withdrawn from the tail vein at 0, 15, 30, 60, and 120 min. *C*: The glucose infusion rates in 3-month-old normal chow diet male pGrb10KO and WT control mice were determined by hyperglycemic clamp experiments (n = 4/group). *D*: Insulin levels of male pGrb10KO and WT littermates during hyperglycemic clamp experiments (n = 4/group). The data represent mean ± SEM. *P < 0.05; **P < 0.01; ***P < 0.001 (one-way repeated-measure ANOVA).

more pancreas weight than that of the WT littermates (Fig. 5*C*). In addition, the male pGrb10KO mice displayed relatively higher plasma insulin levels in response to STZ treatment (Fig. 5*D*) and were protected from STZ-induced loss of β-cells (Fig. 5*E*). Consistent with these findings, TUNEL assays showed that the pGrb10KO mice had lower STZ-induced β-cell apoptosis compared with WT littermates (Fig. 5*F*).

DISCUSSION

Increasing β-cell mass is one of the mechanisms by which glucose homeostasis is maintained in vivo in response to physiological (i.e., growth and gestation) and pathophysiological (i.e., obesity and insulin resistance) stimuli. Unlike other terminally differentiated cell types, pancreatic β-cells retain their ability to proliferate under both physiological and pathophysiological conditions (3). In the progression of diabetes, insulin secretion is increased, and a large amount of the increase in the first stage of this compensation process is due to increased β-cell mass, which is mainly achieved through an increase in β-cell number (24).

The gene encoding for Grb10 is imprinted in mammalian cells, and its expression is defined by its parental origins (25). The maternal allele determines Grb10 expression in all tissues except the brain, and the paternal allele determines Grb10 expression in the brain. Grb10 is expressed in insulin target tissues such as fat and muscle in vivo. The unique structure of the SH2 domain of Grb10 confers its binding specificity to either the insulin or the IGF1R (13) and thus its negative role in insulin or IGF-1 signaling. Ablation of Grb10 in the brain engenders increased social activities of mice (15). Maternal Grb10-deficient animals show enlarged body size and organ size, which enhances insulin signaling and sensitivity (11). In contrast, overexpression of Grb10 in mice led to postnatal growth retardation and insulin resistance (26) or glucose intolerance (27). Dual ablation of Grb10 and Grb14 has no additive effects on insulin signaling and body composition (28).

In the current study, we have used a tissue-specific knockout strategy to demonstrate for the first time that Grb10 plays an important autonomous role in the negative regulation of pancreas mass and β-cell proliferation (Fig. 2*A* and *C*). The pancreas contains multiple cell types including the exocrine (acinar) cells and endocrine cells that included insulin-secreted β-cells. We found that Grb10 disruption, specifically in the pancreas, results in an enlarged pancreas (Fig. 2*A*), which is consistent with previous findings that Grb10 negatively regulates tissue growth (26,29). Our results also showed pancreas-specific knockout of Grb10 increased β-cell mass (Fig. 2*C*). However, because β-cells make up <2% of the pancreas, it is likely that the increased β-cell mass cannot account for the doubling of pancreas mass, suggesting that Grb10 also plays a role in regulating the mass of other cells in the pancreas. It remains to be established whether the enhanced islet mass and β-cell function is due to altered communication between β-cells and neighboring cells. However, some early studies showed that enhanced acinar mass is negatively correlated with insulin secretion and islet mass (30,31). In contrast, we have demonstrated that pancreas-specific deletion of the Grb10 gene protects mice from STZ-induced β-cell apoptosis (Fig. 5). Because Grb10 is a negative regulator of insulin and IGF-1 signaling, it is most likely that the increased β-cell proliferation and enhanced resistance to STZ-induced apoptosis are due to increased insulin/IGF-1 signaling or its mediated downstream signaling events. Consistent with

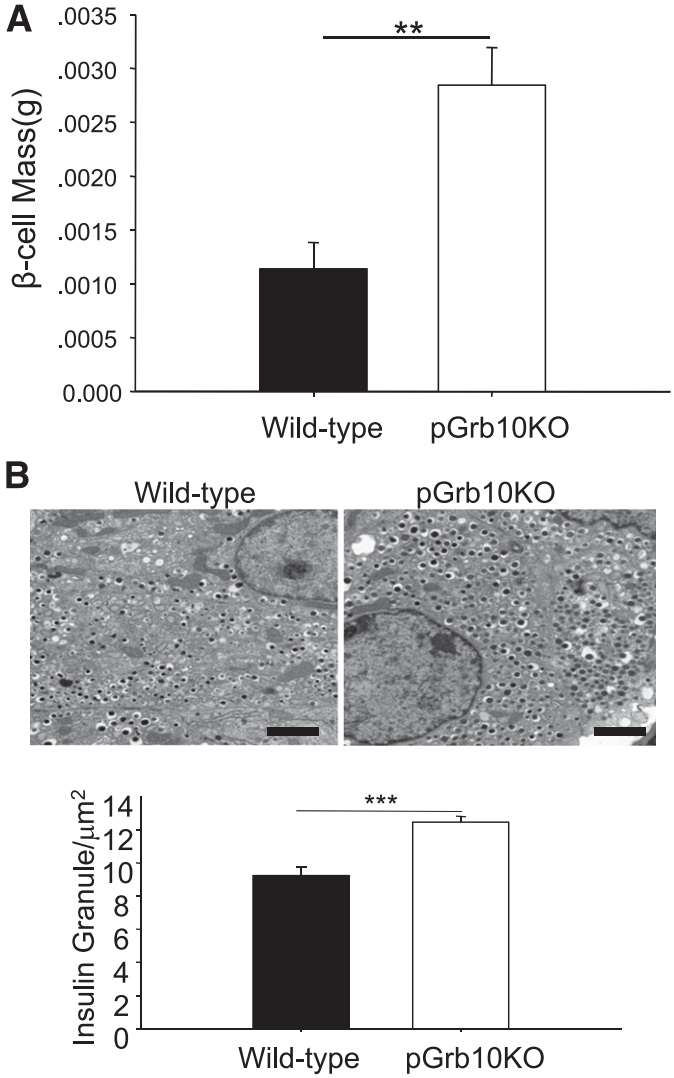

FIG. 4. Pancreatic-specific knockout of Grb10 increased β-cell mass, insulin granule numbers, and insulin/IGF-1 signaling in islets. pGrb10KO mice and WT littermates were fed with 60% HFD for 16 weeks. *A*: Average β-cell mass between male pGrb10KO (n = 4) and WT littermates (n = 3). *B*: Insulin granule numbers in islets of male pGrb10KO (n = 4) and WT littermates (n = 3) were detected. The numbers of docked granules were measured in a cell-surface area of 100 μm^2. Scale bars, 2 μm. The data represent mean ± SEM. *C*: The average β-cell size was analyzed from male pGrb10KO and WT littermates (n = 4/group; >500 cells were counted per slide) using Image-Pro Plus software (Version 5.0; Media Cybernetics, Inc). *D*: Insulin signaling and IGF-1 signaling in β-cell mass. Islets were isolated from HFD-fed male pGrb10KO and WT control mice (n = 5/group), serum starved for 2 h, and treated with insulin (100 nmol/L) or IGF-1 (100 nmol/L) for 30 min. Phosphorylation and the protein levels of Akt Thr^{308} and ERK1/2 Thr^{202}/Tyr^{204} were determined by Western blot using specific antibodies as indicated. *E*: mTOR signaling in β-cell mass. Islets were isolated from male pGrb10KO and

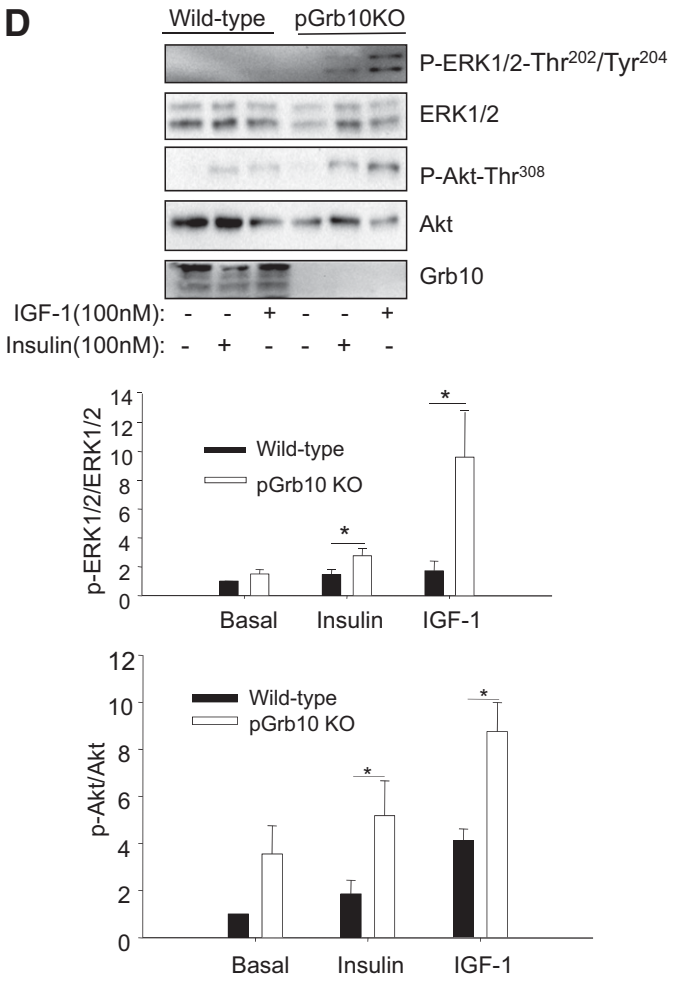

FIG. 4. Continues on next page.

this, we found that insulin- and IGF-1–stimulated phosphorylation of Akt and ERK1/2 was increased in β-cells isolated from pGrb10KO mice compared with that in the WT littermates (Fig. 4*D*). However, it has been shown that β-cell–specific disruption of the genes encoding components in the insulin signaling pathway, including the IR (32), the IGF1R (33,34), phosphoinositide-dependent kinase-1 (34), and Akt (36,37), had little effect on β-cell proliferation. Thus, it is possible that Grb10 negatively regulates other signaling pathways in addition to the insulin/IGF-1 signaling pathways that regulate β-cell proliferation. Consistent with this view, we found that the mTOR signaling pathway is increased in islets of the Grb10 knockout mice compared with WT littermates (Fig. 4*E*). There is some evidence showing that the mTOR signaling pathway plays a key role in the regulation of β-cell mass, survival, and insulin production (40–42). Thus, the increased mTOR signaling may contribute to the enhanced β-cell proliferation

WT control mice (n = 5/group), serum starved for 2 h, and treated with insulin (100 nmol/L) with or without wortmannin (100 nmol/L) for 30 min. Phosphorylation and the protein levels of Akt Thr^{308} and Ser^{473}, ERK1/2 Thr^{202}/Tyr^{204}, p70S6K Thr^{389}, and 4E-BP1 Thr$^{37/46}$ were determined by Western blot using specific antibodies as indicated. Data were quantified by using the Scion Image program (Scion Corporation, Frederick, MD). Black bars, Grb10 flox$^{+/-}$; white bars, pGrb10 KO. The data represent mean ± SEM. *P < 0.05; **P < 0.01; ***P < 0.001 (t test).

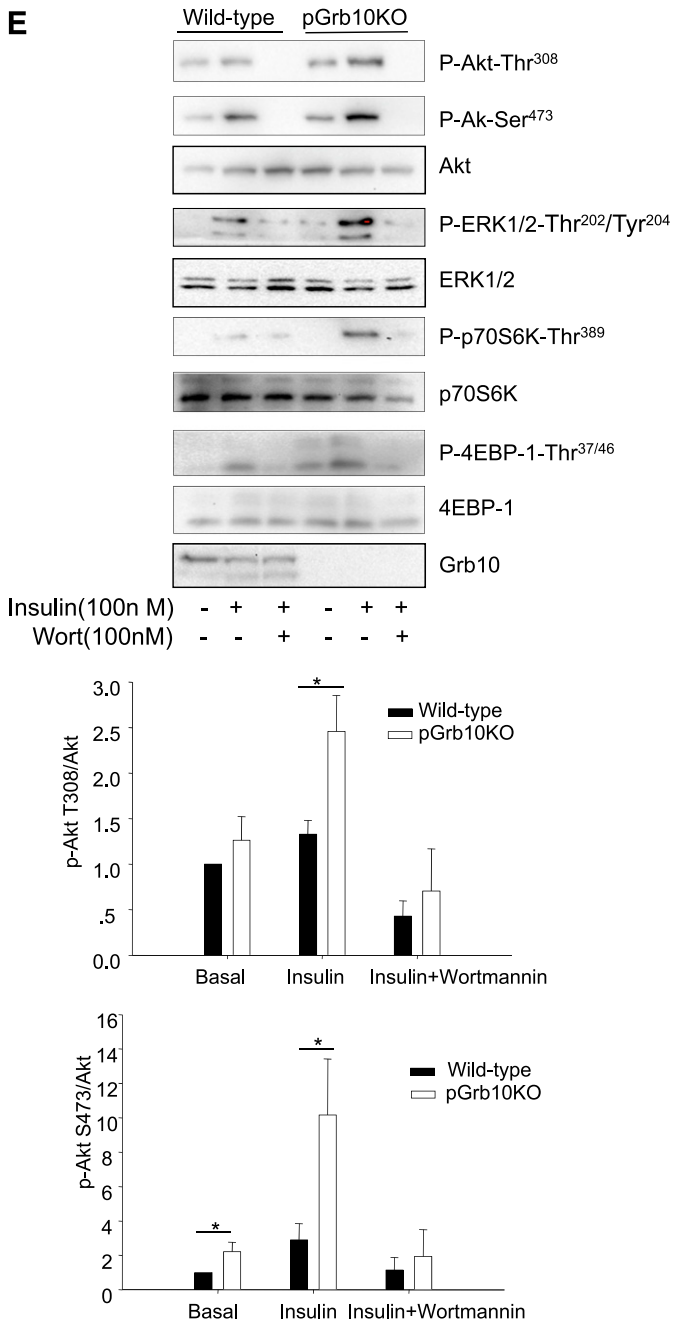

FIG. 4. Continued.

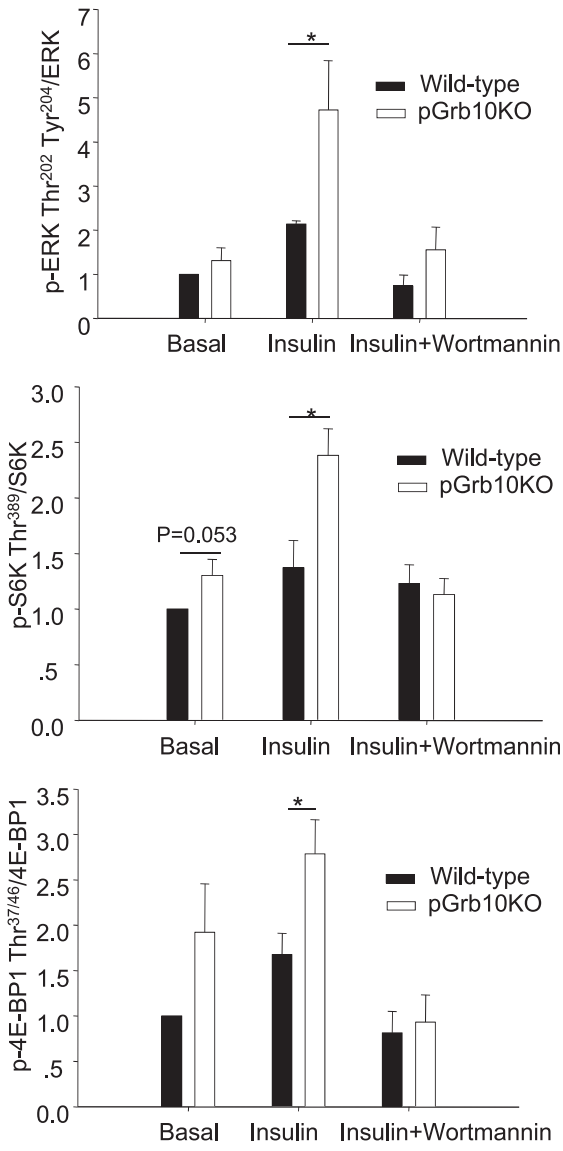

FIG. 4. Continued.

and mass. However, how knocking out of Grb10 increases mTOR signaling remains unknown. Grb10 has recently been identified as a direct substrate of mTOR, and the phosphorylation plays a feedback role in the negative regulation of the phosphatidylinositol 3-kinase (PI3K) and ERK1/2 pathways (38,39). Because mTOR functions downstream of the PI3K/Akt signaling pathway, it is possible that reducing the negative regulation of Grb10 on PI3K/Akt signaling leads to enhanced mTOR signaling. However, it is also possible that Grb10 may have a direct effect on mTOR. We are currently investigating these possibilities.

It is well-established that β-cells have low antioxidant protection capability and are prone to apoptosis induced by oxidative stress and inflammation (43,44). In fact, pancreatic β-cell apoptosis has been recognized as a key event in type 1 diabetes (45). Our results show that pancreas-specific disruption of Grb10 protects mice from STZ-induced apoptosis (Fig. 5*F*). Because Grb10 is highly expressed in pancreas (11) and islets (Fig. 1*C* and *D*), and this protein negatively regulates insulin/IGF-1 signaling in cells (7–9) and in vivo (10,11), which are known to exert an antiapoptotic function, it is possible that the high expression level of Grb10 in β-cells plays a causative role in the low antioxidant protection capability. Thus, reducing Grb10 expression in β-cells would provide an approach to reduce the rate of oxidative stress-induced apoptosis.

Our results show that knockout of Grb10 enhances insulin signaling in isolated islets and protects mice against STZ-induced apoptosis (Figs. 4*D* and 5*F*), suggesting that Grb10 has an autonomous effect on β-cell function and survival. However, the finding that Grb10 is expressed not only in insulin positive β-cells but also in other cells of the islets (Fig. 1*D*) suggests that Grb10 may have an additional function. It is well-established that the pancreas contains multiple cell types including the exocrine (acinar) cells and endocrine cells such as the glucagon-producing α-cells, the insulin-producing β-cells, the somatostatin-producing δ

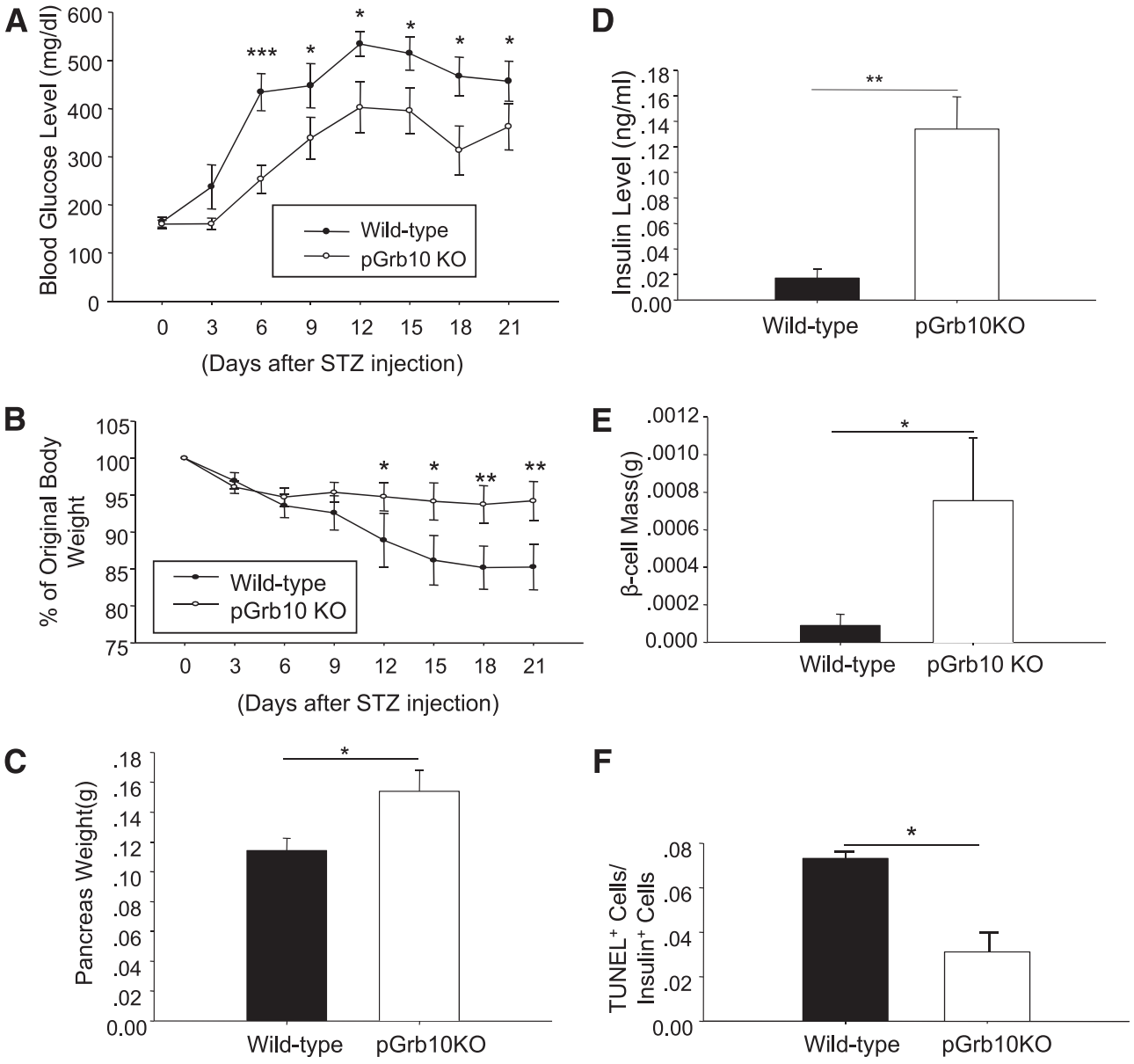

FIG. 5. Pancreatic-specific knockout of Grb10 enhances resistance to STZ-induced diabetes in mice. Male pGrb10KO and WT control mice (2 months old) were treated with STZ (75 mg/kg) for 5 days. Blood glucose levels (*A*) and body weight (*B*) were measured in WT (n = 8) and pGrb10KO (n = 11) mice every 3 days at the same time point (12 P.M. each day) after STZ treatment. Data are shown as mean ± SEM. *P < 0.05; **P < 0.01; ***P < 0.001 (one-way repeated-measure ANOVA). *C*: pGrb10KO (n = 6) and WT (n = 8) mice were treated with STZ for 22 days and killed. Pancreases were isolated and weighed. *D*: pGrb10KO mice (n = 4) and WT littermates (n = 3) were treated with STZ for 22 days and then killed. Serum was collected for insulin measurement. *E*: Average β-cell mass between pGrb10KO (n = 4) and WT littermates (n = 3). *F*: Cell apoptosis rate was analyzed by TUNEL assay between pGrb10KO mice (n = 4) and WT littermates (n = 3). Mice were injected with STZ twice daily (0 and 24 h) and killed 24 h later. More than 2,500 insulin-positive cells were counted per mice. Black bars, Grb10 flox$^{+/-}$; white bars, pGrb10 KO. Data are shown as mean ± SEM. *P < 0.05; **P < 0.01 (t test).

cells, and the pancreatic polypeptide- and ghrelin-producing ε cells (46). A number of studies have demonstrated that hormones and other paracrine factors from neighboring cells play critical roles in regulating insulin release from β-cells (47–49). Although it remains to be established whether Grb10 is expressed in all of these cells and is involved in the communication between β-cells and neighboring pancreatic cells, it is possible that in addition to an autonomous mechanism, Grb10 may regulate β-cell function and survival by a nonautonomous mechanism in vivo. Further studies will be needed to test this possibility.

In summary, our study has identified Grb10 as a key negative regulator of β-cell proliferation, function, and survival. β-Cell failure, which is largely due to impairment in cell proliferation and increased cell death, is a key component in the pathogenesis of both type 1 and type 2 diabetes. Therefore, increasing β-cell mass from endogenous sources represents highly significant research area for developing specific therapeutic treatment for human diabetes. Approaches to suppress Grb10 function in β-cells may thus be an effective strategy for treating type 1 and type 2 diabetes.

ACKNOWLEDGMENTS

This study was partly supported by grants from the National Nature Science Foundation of China (81130015

and 81000316 to J.Z. and F.L.), National Institutes of Health grants NIMH 076929 (to X.-Y.L.), AG-030979, DK-80157, and DK-089229 (to N.M.).

No potential conflicts of interest relevant to this article were reported.

J.Z. designed and performed research, analyzed data, and wrote the manuscript. N.Z., N.M., and R.A.D. helped with the clamp study. M.L., L.Z., W.H., Z.X., and J.L. performed research. X.L. and J.M.C. helped in the generation of the Grb10 floxed mice. Z.Z. and X.-Y.L. analyzed data. F.L. supervised the project, designed the research, analyzed data, and wrote the manuscript. F.L. is the guarantor of this work and, as such, had full access to all the data in the study and takes responsibility for the integrity of the data and the accuracy of the data analysis.

Parts of this study were presented in abstract form at the 71st Scientific Sessions of the American Diabetes Association, San Diego, California, 24–28 June 2011.

REFERENCES

1. Ehrmann DA, Sturis J, Byrne MM, Karrison T, Rosenfield RL, Polonsky KS. Insulin secretory defects in polycystic ovary syndrome. Relationship to insulin sensitivity and family history of non-insulin-dependent diabetes mellitus. J Clin Invest 1995;96:520–527
2. Ward WK, Bolgiano DC, McKnight B, Halter JB, Porte D Jr. Diminished B cell secretory capacity in patients with noninsulin-dependent diabetes mellitus. J Clin Invest 1984;74:1318–1328
3. Bonner-Weir S. Life and death of the pancreatic beta cells. Trends Endocrinol Metab 2000;11:375–378
4. Butler AE, Janson J, Bonner-Weir S, Ritzel R, Rizza RA, Butler PC. Beta-cell deficit and increased beta-cell apoptosis in humans with type 2 diabetes. Diabetes 2003;52:102–110
5. Holt LJ, Siddle K. Grb10 and Grb14: enigmatic regulators of insulin action—and more? Biochem J 2005;388:393–406
6. Lim MA, Riedel H, Liu F. Grb10: more than a simple adaptor protein. Front Biosci 2004;9:387–403
7. Frantz JD, Giorgetti-Peraldi S, Ottinger EA, Shoelson SE. Human GRB-IRbeta/GRB10. Splice variants of an insulin and growth factor receptor-binding protein with PH and SH2 domains. J Biol Chem 1997;272:2659–2667
8. Liu F, Roth RA. Grb-IR: a SH2-domain-containing protein that binds to the insulin receptor and inhibits its function. Proc Natl Acad Sci USA 1995;92:10287–10291
9. O'Neill TJ, Rose DW, Pillay TS, Hotta K, Olefsky JM, Gustafson TA. Interaction of a GRB-IR splice variant (a human GRB10 homolog) with the insulin and insulin-like growth factor I receptors. Evidence for a role in mitogenic signaling. J Biol Chem 1996;271:22506–22513
10. Smith FM, Holt LJ, Garfield AS, et al. Mice with a disruption of the imprinted Grb10 gene exhibit altered body composition, glucose homeostasis, and insulin signaling during postnatal life. Mol Cell Biol 2007;27:5871–5886
11. Wang L, Balas B, Christ-Roberts CY, et al. Peripheral disruption of the Grb10 gene enhances insulin signaling and sensitivity in vivo. Mol Cell Biol 2007;27:6497–6505
12. Dong LQ, Farris S, Christal J, Liu F. Site-directed mutagenesis and yeast two-hybrid studies of the insulin and insulin-like growth factor-1 receptors: the Src homology-2 domain-containing protein hGrb10 binds to the autophosphorylated tyrosine residues in the kinase domain of the insulin receptor. Mol Endocrinol 1997;11:1757–1765
13. Stein EG, Ghirlando R, Hubbard SR. Structural basis for dimerization of the Grb10 Src homology 2 domain. Implications for ligand specificity. J Biol Chem 2003;278:13257–13264
14. Stein EG, Gustafson TA, Hubbard SR. The BPS domain of Grb10 inhibits the catalytic activity of the insulin and IGF1 receptors. FEBS Lett 2001;493:106–111
15. Garfield AS, Cowley M, Smith FM, et al. Distinct physiological and behavioural functions for parental alleles of imprinted Grb10. Nature 2011;469:534–538
16. Hikichi T, Kohda T, Kaneko-Ishino T, Ishino F. Imprinting regulation of the murine Meg1/Grb10 and human GRB10 genes; roles of brain-specific promoters and mouse-specific CTCF-binding sites. Nucleic Acids Res 2003;31:1398–1406
17. Bernal-Mizrachi E, Wen W, Stahlhut S, Welling CM, Permutt MA. Islet beta cell expression of constitutively active Akt1/PKB alpha induces striking hypertrophy, hyperplasia, and hyperinsulinemia. J Clin Invest 2001;108:1631–1638
18. Martinez SC, Cras-Méneur C, Bernal-Mizrachi E, Permutt MA. Glucose regulates Foxo1 through insulin receptor signaling in the pancreatic islet beta-cell. Diabetes 2006;55:1581–1591
19. Hennige AM, Burks DJ, Ozcan U, et al. Upregulation of insulin receptor substrate-2 in pancreatic beta cells prevents diabetes. J Clin Invest 2003;112:1521–1532
20. Withers DJ, Burks DJ, Towery HH, Altamuro SL, Flint CL, White MF. Irs-2 coordinates Igf-1 receptor-mediated beta-cell development and peripheral insulin signalling. Nat Genet 1999;23:32–40
21. Hull RL, Kodama K, Utzschneider KM, Carr DB, Prigeon RL, Kahn SE. Dietary-fat-induced obesity in mice results in beta cell hyperplasia but not increased insulin release: evidence for specificity of impaired beta cell adaptation. Diabetologia 2005;48:1350–1358
22. Bonner-Weir S. beta-cell turnover: its assessment and implications. Diabetes 2001;50(Suppl. 1):S20–S24
23. Liu JL, Coschigano KT, Robertson K, et al. Disruption of growth hormone receptor gene causes diminished pancreatic islet size and increased insulin sensitivity in mice. Am J Physiol Endocrinol Metab 2004;287:E405–E413
24. Weir GC, Bonner-Weir S. Five stages of evolving beta-cell dysfunction during progression to diabetes. Diabetes 2004;53(Suppl. 3):S16–S21
25. Sanz LA, Chamberlain S, Sabourin JC, et al. A mono-allelic bivalent chromatin domain controls tissue-specific imprinting at Grb10. EMBO J 2008;27:2523–2532
26. Shiura H, Miyoshi N, Konishi A, et al. Meg1/Grb10 overexpression causes postnatal growth retardation and insulin resistance via negative modulation of the IGF1R and IR cascades. Biochem Biophys Res Commun 2005;329:909–916
27. Yamamoto Y, Ishino F, Kaneko-Ishino T, et al. Type 2 diabetes mellitus in a non-obese mouse model induced by Meg1/Grb10 overexpression. Exp Anim 2008;57:385–395
28. Holt LJ, Lyons RJ, Ryan AS, et al. Dual ablation of Grb10 and Grb14 in mice reveals their combined role in regulation of insulin signaling and glucose homeostasis. Mol Endocrinol 2009;23:1406–1414
29. Charalambous M, Smith FM, Bennett WR, Crew TE, Mackenzie F, Ward A. Disruption of the imprinted Grb10 gene leads to disproportionate overgrowth by an Igf2-independent mechanism. Proc Natl Acad Sci USA 2003;100:8292–8297
30. McEvoy RC, Hegre OD. Foetal rat pancreas in organ culture: effects of media supplementation with various steroid hormones on the acinar and islet components. Differentiation 1976;6:105–111
31. Rall L, Pictet R, Githens S, Rutter WJ. Glucocorticoids modulate the in vitro development of the embryonic rat pancreas. J Cell Biol 1977;75:398–409
32. Kulkarni RN, Brüning JC, Winnay JN, Postic C, Magnuson MA, Kahn CR. Tissue-specific knockout of the insulin receptor in pancreatic beta cells creates an insulin secretory defect similar to that in type 2 diabetes. Cell 1999;96:329–339
33. Kulkarni RN, Holzenberger M, Shih DQ, et al. beta-cell-specific deletion of the Igf1 receptor leads to hyperinsulinemia and glucose intolerance but does not alter beta-cell mass. Nat Genet 2002;31:111–115
34. Xuan S, Kitamura T, Nakae J, et al. Defective insulin secretion in pancreatic beta cells lacking type 1 IGF receptor. J Clin Invest 2002;110:1011–1019
35. Hashimoto N, Kido Y, Uchida T, et al. Ablation of PDK1 in pancreatic beta cells induces diabetes as a result of loss of beta cell mass. Nat Genet 2006;38:589–593
36. Bernal-Mizrachi E, Fatrai S, Johnson JD, et al. Defective insulin secretion and increased susceptibility to experimental diabetes are induced by reduced Akt activity in pancreatic islet beta cells. J Clin Invest 2004;114:928–936
37. Cho H, Mu J, Kim JK, et al. Insulin resistance and a diabetes mellitus-like syndrome in mice lacking the protein kinase Akt2 (PKB beta). Science 2001;292:1728–1731
38. Hsu PP, Kang SA, Rameseder J, et al. The mTOR-regulated phosphoproteome reveals a mechanism of mTORC1-mediated inhibition of growth factor signaling. Science 2011;332:1317–1322
39. Yu Y, Yoon SO, Poulogiannis G, et al. Phosphoproteomic analysis identifies Grb10 as an mTORC1 substrate that negatively regulates insulin signaling. Science 2011;332:1322–1326
40. Fraenkel M, Ketzinel-Gilad M, Ariav Y, et al. mTOR inhibition by rapamycin prevents beta-cell adaptation to hyperglycemia and exacerbates the metabolic state in type 2 diabetes. Diabetes 2008;57:945–957
41. Mori H, Inoki K, Opland D, et al. Critical roles for the TSC-mTOR pathway in β-cell function. Am J Physiol Endocrinol Metab 2009;297:E1013–E1022

42. Balcazar N, Sathyamurthy A, Elghazi L, et al. mTORC1 activation regulates beta-cell mass and proliferation by modulation of cyclin D2 synthesis and stability. J Biol Chem 2009;284:7832–7842
43. Grankvist K, Marklund SL, Täljedal IB. CuZn-superoxide dismutase, Mn-superoxide dismutase, catalase and glutathione peroxidase in pancreatic islets and other tissues in the mouse. Biochem J 1981;199:393–398
44. Tiedge M, Lortz S, Drinkgern J, Lenzen S. Relation between antioxidant enzyme gene expression and antioxidative defense status of insulin-producing cells. Diabetes 1997;46:1733–1742
45. Mathis D, Vence L, Benoist C. beta-Cell death during progression to diabetes. Nature 2001;414:792–798
46. Elayat AA, el-Naggar MM, Tahir M. An immunocytochemical and morphometric study of the rat pancreatic islets. J Anat 1995;186:629–637
47. Kawamori D, Kurpad AJ, Hu J, et al. Insulin signaling in alpha cells modulates glucagon secretion in vivo. Cell Metab 2009;9:350–361
48. Prasadan K, Daume E, Preuett B, et al. Glucagon is required for early insulin-positive differentiation in the developing mouse pancreas. Diabetes 2002;51:3229–3236
49. Vuguin PM, Kedees MH, Cui L, et al. Ablation of the glucagon receptor gene increases fetal lethality and produces alterations in islet development and maturation. Endocrinology 2006;147:3995–4006